Silver Hydro Sodalite $[Ag_3(H_2O)_4]_2[Al_3Si_3O_{12}]_2$: Synthesis and Structure Determination by Combination of X-ray Rietveld Refinement, Thermogravimetry, FT-IR, and ^{1}H-MAS NMR Spectroscopy

Stefanie Eiden-Aßmann,*[a] Andreas M. Schneider,[b] Peter Behrens,[b] Guenter Engelhardt,[c] Hugo Mändar,[d] and Juergen Felsche[e]

Keywords: Silver / Sodalite / Ion exchange / Rietveld refinement

Sodium hydro sodalite $[Na_3(H_2O)_4]_2[Al_3Si_3O_{12}]_2$ was subjected to ion exchange with aqueous $AgNO_3$ solutions to yield silver hydro sodalite $[Ag_3(H_2O)_4]_2[Al_3Si_3O_{12}]_2$. A Rietveld structure refinement of the silver hydro sodalite structure based on powder X-ray diffraction data recorded at room temperature (cubic, a = 8.950 Å, space group P-43n) led to a model where three silver cations form a triangle nearly parallel to a four-membered ring of the sodalite cage. In combination with the four water molecules, a disorder model $[Ag_3(\mu\text{-}H_2O)_2(H_2O)_2]^{3+}$ is suggested. This structural arrangement is clearly different from that found in sodium hydro sodalite. Whereas the sodium hydro sodalite structure is dominated by cation–water interactions, the silver hydro sodalite structure reflects strong interactions between the cations and the oxygen atoms of the framework, strong interactions between the water molecules, but only weak ones between the cations and water molecules. In addition, weak $Ag^+\cdots Ag^+$ interactions may play a role. ^{1}H MAS NMR spectra show that the hydrogen atoms (which were not found in the Rietveld analysis) of the water molecules are involved in hydrogen bonding of different strengths and dynamics.

Introduction

The framework of 1:1 aluminosilicate sodalites consists of a periodic array of space-filling $[4^66^8]$ polyhedra (β cages) formed by a network of alternating and corner-sharing SiO_4 and AlO_4 tetrahedra with a unit-cell content of $[Al_3Si_3O_{12}]_2^{6-}$.[1] In addition to cations M^+ compensating for the negative charge of the framework, the β cages may contain a large variety of encapsulated salts M^+A^-, hydroxides M^+OH^-, and/or water molecules. The general unit-cell composition of aluminosilicate sodalites can thus be given as $[M_{3+x}A_x(H_2O)_n]_2[Al_3Si_3O_{12}]_2$, where M and A are singly charged cations and anions, respectively. Owing to their structural relationship with the well-known and industrially important A-, X-, and Y-type zeolites, sodalites have been considered as model systems in order to investigate the various kinds of host–guest interactions, static-statistical and/or dynamical guest disorder phenomena, and structural-phase transitions.[2,3]

In addition, sodalites have also attracted considerable attention because of their intracage reaction chemistry and their interesting material properties such as cathodochromism, photochromism, and ion conduction. They are also considered as periodic host matrices for the spatial organization of quantum-sized semiconductor clusters and cluster arrays.[4] Phenomena such as blue shifts in optical absorption edges have been observed for aluminosilicate sodalites that contain silver salts[5] and have been interpreted as quantum-size effects. Stein et. al[6] reported a silver oxalato sodalite $[Ag_8(C_2O_4)][Al_3Si_3O_{12}]$ that can be reversibly marked and erased with a laser beam for many cycles. A large number of different silver sodalites have been synthesized[7] and some of them have been structurally characterized by Rietveld refinements of X-ray diffraction data.[8,9] Notably, the refinement of the structure of the silver hydro sodalite (SHS), i.e. a sodalite containing only Ag^+ ions and water molecules in its cages, did not converge easily and stopped at relatively high R values with the structural model reported.[10] The structure of anhydrous silver sodalite $[Ag_3]_2[Al_3Si_3O_{12}]_2$ was studied in detail at different temperatures and with regard to a phase transition.[11]

As part of our investigation into the synthesis, structure and properties of aluminosilicate sodalites containing heavy metal cations,[11,12] we have studied the ion exchange of the well-characterized sodium hydro sodalite $[Na_3(H_2O)_4]_2[Al_3Si_3O_{12}]_2$ with aqueous $AgNO_3$ solution. This paper reports the characterization of SHS by means of a Rietveld structure refinement based on powder X-ray diffraction, as well as by ^{1}H MAS NMR, ^{29}Si MAS NMR and FT-IR spectroscopy and by thermal analysis.

Results

Treatment of the sodium hydro sodalite $[Na_3(H_2O)_4]_2[Al_3Si_3O_{12}]_2$ with an aqueous solution of $AgNO_3$ (1 M) at

[a] Universität Konstanz, Fachbereich für Physik, 78464 Konstanz, Germany
[b] Universität Hannover, Institut für Anorganische Chemie, 30167 Hannover, Germany
[c] Universität Stuttgart, Institut für Technische Chemie, 70550 Stuttgart, Germany
[d] University of Tartu, Dept. of Physics, 51010 Tartu, Estonia
[e] Universität Konstanz, Fachbereich für Chemie, 78464 Konstanz, Germany

  1434–1948/01/0606–1527 $ 17.50+.50/0

383 K affords complete exchange of all sodium cations with silver cations, with retention of the sodalite host structure. The combination of analytical techniques employed by us suggests that the idealized chemical composition $[Ag_3(H_2O)_4]_2[Al_3Si_3O_{12}]_2$ is present in the product phase. Powder X-ray photographs showed that the crystallinity of the reactant sodalite is essentially preserved during ion exchange, and that the product is a single-phase material. No amorphous by-product was visible on scanning electron micrographs, therefore all the analytic data refer to the crystalline compound. The degree of ion exchange, determined by flame photometry and titration according to the method of Volhard, amounts to 95%.

The ^{29}Si MAS NMR spectrum (Figure 1) shows a narrow line at $\delta = -85.4$, indicating that the ordered 1:1 aluminosilicate framework is retained after the ion-exchange reaction.[13]

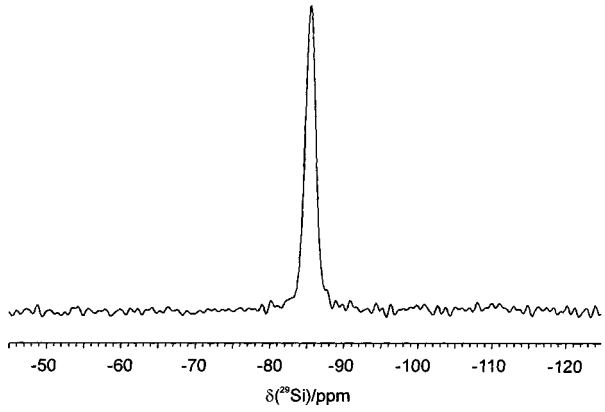

Figure 1. ^{29}Si MAS NMR spectrum of silver hydro sodalite

Thermal analysis (Figure 2) clearly demonstrates the presence of eight water molecules per unit cell. These water molecules are released from the SHS in a two-step reaction, in the temperature range from 400 to 600 K. The IR spectrum exhibits broad bands assigned to H_2O stretching vibrations in the range between 3000 and 3600 cm^{-1}, typical for water molecules involved in hydrogen bonding. In addition, a relatively narrow band appears at 1660 cm^{-1}, assigned to the H_2O deformation mode. The bands below 1200 cm^{-1} originate from framework vibrations.[14]

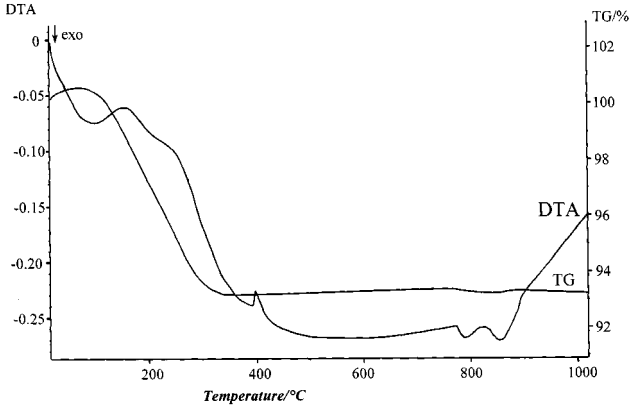

Figure 2. Simultaneous thermal analysis (TG/DTG/DTA) of silver hydro sodalite $[Ag_3(H_2O)_4]_2[Al_3Si_3O_{12}]_2$

Crystal Structure

Atomic coordinates and selected structural data of $[Ag_3(H_2O)_4]_2[Al_3Si_3O_{12}]_2$, as obtained from Rietveld refinement, are summarized in Table 1, Table 2, and Table 3.

Table 1. Fractional atomic coordinates, displacement parameters U and population parameter (PP) for $[Ag_3(H_2O)_4]_2[Al_3Si_3O_{12}]_2$ (data set 1)

Atom	Wyckoff position	x	y	z	U_{iso} [Å^2]	PP
Si	6*c*	1/4	1/2	0	0.0001(6)[a]	1.0
Al	6*d*	1/4	0	1/2	0.0001[a]	1.0
O1	24*i*	0.1390(6)	0.1481(7)	0.4424(5)	0.002(2)	1.0
Ag1	8*e*	0.1723(2)	*x*	*x*	0.032(5)[a]	0.75[b]
Ag2	8e	0.3081(4)	*x*	*x*	0.032[a]	0.25
O2	8*e*	0.3968(7)	*x*	*x*	0.069(7)	0.75

[a] U(Si) and U(Al) were refined as constrained parameters, U(Al) = U(Si). − U(Ag1) and U(Ag2) were refined as constrained parameters, U(Ag1) = U(Ag2). − [b] PP(Ag1), PP(Ag2) and PP(O2) were treated as described in the text during the refinement procedure.

Table 2. Fractional atomic coordinates, displacement parameters U and population parameter (PP) for $[Ag_3(H_2O)_4]_2[Al_3Si_3O_{12}]_2$ (data set 2)

Atom	Wyckoff position	x	Y	z	U	PP
Si	6*c*	1/4	1/2	0	0.0044(6)[a]	1.0
Al	6*d*	1/4	0	1/2	0.0044[a]	1.0
O1	24*i*	0.1392(6)	0.1473(6)	0.4420(3)	0.006(1)	1.0
Ag1	8*e*	0.1729(1)	*x*	*x*	0.0481(4)[a]	0.5[b]
Ag2	8e	0.3103(4)	*x*	*x*	0.0481[a]	0.25[b]
O2	8*e*	0.4000(3)	*x*	*x*	0.054(6)	0.75[b]

[a] U(Si) and U(Al) were refined as dependent parameters, U(Al) = U(Si). − U(Ag1) and U(Ag2) were refined as dependent parameters, U(Ag1) = U(Ag2). − [b] (Ag1), PP(Ag2) and PP(O2) were treated during the refinement procedure as described in the text.

Structural details are shown in Figure 3. The results are practically identical for both data sets, although some small deviations occur. In both refinement procedures, we were able to identify the positions of the silicon, aluminium, and oxygen atoms of the framework, the positions of the six silver cations and the positions of six out of the eight oxygen atoms of the occluded water molecules (Figure 3, **a** and **b**). In both cases it was not possible to determine the positions of the oxygen atoms of the two remaining water molecules. We assume that these are situated on a Wyckoff 8*e* position with a population parameter of 25%, close to the Wyckoff 8*e* position of the silver cation Ag1. The introduction of an oxygen atom O3 at this position during the re-

Table 3. Selected interatomic distances [Å] and angles [°] for $[Ag_3(H_2O)_4]_2[Al_3Si_3O_{12}]_2$

Host Structure					
	data set 1	data set 2		data set 1	data set 2
Al−O1	1.745(6)	1.739(5)	Si−O1	1.635(6)	1.642(6)
O1−Al−O1 (4x)	109.1(2)	109.2(2)	O1−Si−O1 (4x)	108.3(3)	108.5(3)
O1−Al−O1 (2x)	110.1(3)	110.0(3)	O1−Si−O1 (2x)	111.8(3)	111.5(3)
Al−O1−Si	140.5(2)				
Silver and oxygen coordination					
	Data set 1	Data set 2		Data set 1	Data set 2
Ag1−O1	2.459(5)	2.452(3)	Ag2−O1	2.419(7)	2.435(6)
	3.127(6)	3.130(4)		3.349(6)	3.750(6)
Ag1−O2	2.641(7)	2.625(3)	Ag2−O2	3.840(7)	3.774(5)
	3.500(7)	3.540(3)			
Ag1−Ag2	3.287(4)	3.270(4)			

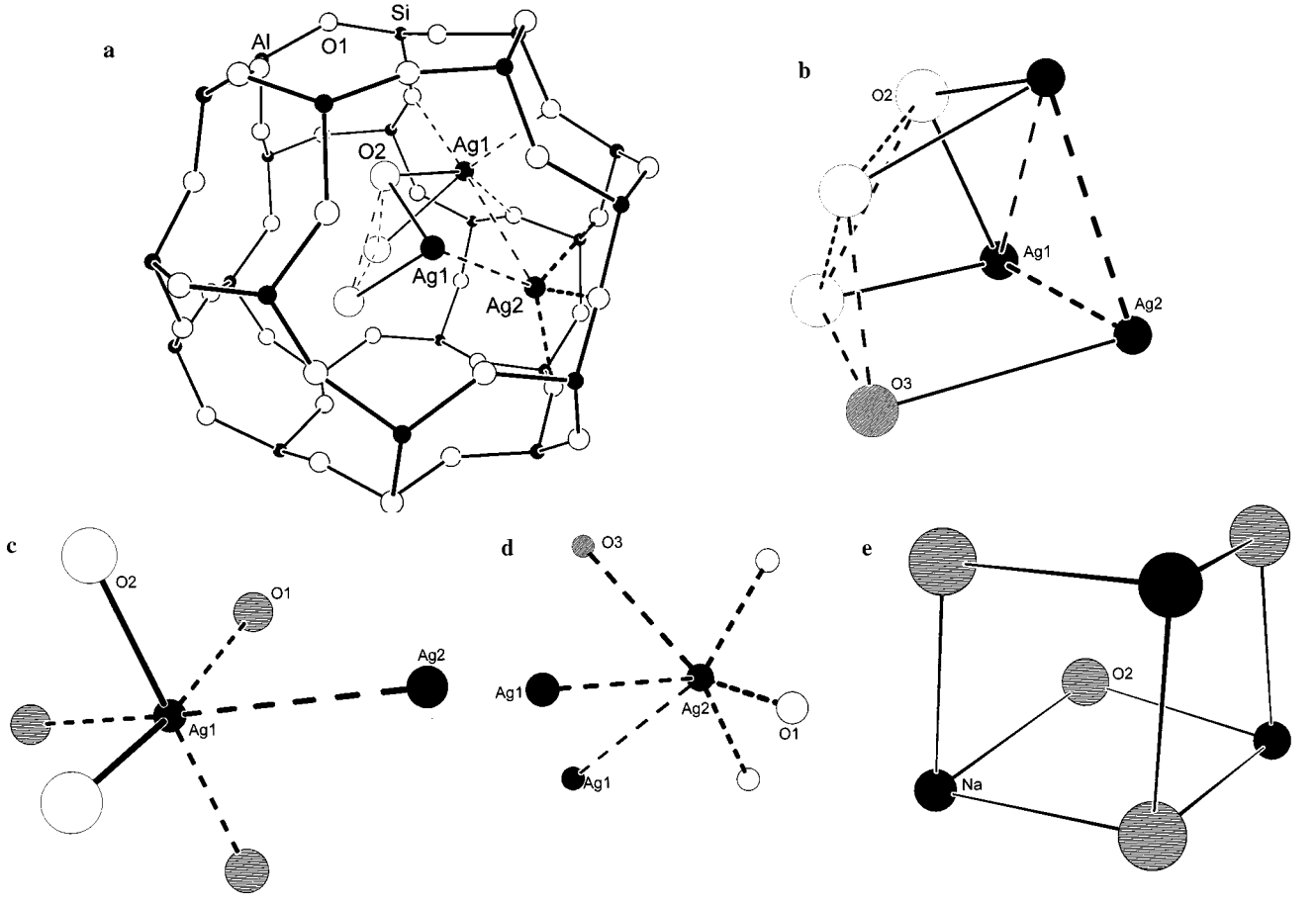

Figure 3. The crystal structure of silver hydro sodalite according to the Rietveld refinement. **a**: The sodalite cage with the positions of the Ag1 and the Ag2 atoms as well as those of O2 atoms. **b**: The arrangement of the intracage atoms (note that the position of O3 could not be refined); full lines indicate Ag−O coordination, dashed lines indicate weak interactions (hydrogen bonding, Ag···Ag interactions); **c**: The (3+2+1) coordination of Ag1; **d**: The (3+1+2) coordination of Ag2; **e**: The arrangement of intracage atoms in sodium hydro sodalite

finement led to unreasonably short distances of d(O2−O3) ≈ 1.85 Å. Therefore the remaining oxygen atoms were neglected. We are conscious of the fact that this omission might lead to results which do not represent the true structure. Nevertheless, there are convincing arguments that the model which we will present is essentially correct.

Owing to the similar results of the two data sets, only the results of the refinement of the second data set will be discussed. Interatomic distances and angles of the framework structure were found mainly in the expected range. Silver cations were found at two 8*e*-Wyckoff positions. The population parameters of 50% for Ag1 and 25% for Ag2 were retained during the refinement procedure, but were relaxed several times to examine their behaviour and to ensure that no large deviations from the fixed values would occur. They were set back to their original values of 50% and 25%, respectively, after such test cycles. The occurrence of two Ag positions and the refined population parameters for the occluded silver cations and oxygen atoms of water molecules may be explained with a disorder model.

This disorder model of the non-framework atoms may be derived from the shortest distances to obtain a reasonable coordination sphere. In general, each sodalite cage contains a $[Ag_3(OH_2)_4]^{3+}$ cluster as a guest species, which is also found in silver-exchanged zeolite A.[15] The same number of metal cations and water molecules are also present as a $[Na_3(H_2O)_4]^{3+}$ cluster in $[Na_3(H_2O)_4]_2[Al_3Si_3O_{12}]_2$. However, there are significant differences between these two compounds and $[Ag_3(H_2O)_4]_2[Al_3Si_3O_{12}]_2$. Whereas in silver zeolite A and in $[Na_3(H_2O)_4]_2[Al_3Si_3O_{12}]_2$ the cations and water molecules are detected at one Wyckoff 8e position each (Figure 3, **e**), leading to coordination of the cations by three framework oxygen atoms and three water molecules, the arrangement is significantly different in SHS.

In SHS, each silver cation Ag1 is surrounded by three oxygen atoms of the framework [d(Ag1−O1) = 2.452(3) Å] and two oxygen atoms of water molecules [d(Ag1−O2) = 2.625(3) Å]. In addition, a relatively short contact between the silver cations Ag1 and Ag2 is found [d(Ag1−Ag2) = 3.270(4) Å], resulting in a sixfold (3+2+1) coordination (Figure 3, **c**). A distance of d(Ag2−O1) = 2.435(6) Å is found for the contacts between the silver cations Ag2 and the framework oxygen atoms. In addition to three framework oxygen atoms, this cation is coordinated to two neighbouring silver cations Ag1, and to one oxygen atom of an occluded water molecule (Figure 3, **d**), although the position of the oxygen atom of this water molecule could not be determined unequivocally. It is likely to be close to the position of the Ag1 silver cation with a population parameter of 25%, as mentioned before. Taken together, this results in a sixfold (3+1+2) coordination. Combining these results, we find an isosceles silver triangle composed of two Ag1 cations and one Ag2 cation, which is surrounded by oxygen atoms of the framework as well as of the occluded water molecules (Figure 3, **b**). The $[Ag_3]$ triangle is a very common motif in silver compounds, e.g. in dehydrated silver zeolite A[15] as well as in many ternary silver oxides.[16] Owing to the population parameters, the triangles show a fourfold orientational disorder with respect to the β-cage. Snapshot pictures of the structural model are given in Figure 3.

Oxygen atoms of the occluded water molecules are found on the corners of a tetrahedron (Wyckoff 8*e* position) with a population of 75%. Within the tetrahedron, the distance between two oxygen atoms was found to be d(O2−O2) = 2.545(4) Å, indicating the prevalence of strong hydrogen bonding between the water molecules at this position (Figure 3, **b**). The distance to the nearest oxygen atom of the host structure is d(O1−O2) = 3.24 Å, which is quite large but might still be indicative of weak hydrogen bonding between the occluded water molecules and the framework oxygen atoms. This is supported by the results of the ^{1}H NMR experiments (Figure 4). Two different types of hydrogen atoms were found. We ascribe these to hydrogen atoms involved in the stronger hydrogen bonding within the cluster of occluded water molecules (type 1, δ = 6), and hydrogen atoms involved in contacts from the water molecules to the framework oxygen atoms (type 2, δ = 5).

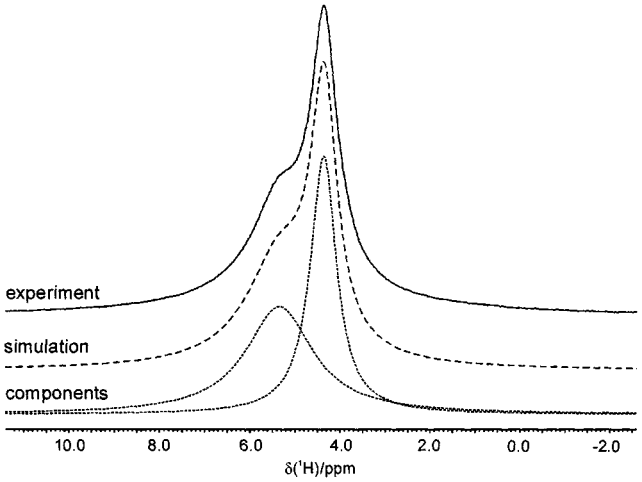

Figure 4. ^{1}H MAS NMR spectrum of silver hydro sodalite

The results of temperature-dependent ^{1}H MAS NMR spectroscopic investigations (Figure 5) indicate that at temperatures above 383 K, the dynamics of the water molecules

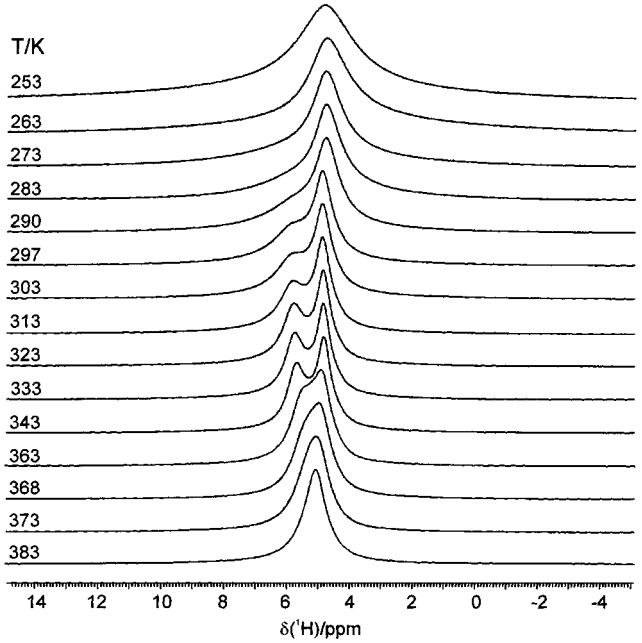

Figure 5. ^{1}H MAS NMR spectra of silver hydro sodalite at different temperatures

inside the sodalite cage is so fast, that the different types of hydrogen atoms become indistinguishable. In the temperature range from 368 K to 290 K, two separate signals were visible. At lower temperatures, one broad, slightly asymmetric peak was observed, and simulation of the spectra clearly shows the presence of two overlapping signals.

Discussion

Our studies demonstrate that the arrangement of the non-framework species in aluminosilicate silver hydro sodalite SHS is considerably different to the corresponding structures in its sodium analogue $[Na_3(H_2O)_4]_2[Al_3Si_3O_{12}]_2$[17] and in the sodalite cages of hydrated silver zeolite A.[15] In all cases, one sodalite cage contains three metal cations and four water molecules. In the sodium hydro sodalite and in the silver zeolite, the metal ions are positioned at the corners of a tetrahedron, with a 75% occupancy and a corresponding disorder between the different cages. The oxygen atoms of the water molecules form another tetrahedron. The principle arrangement of the water molecules is similar in SHS, but the arrangement of the silver cations is different. They are positioned at the corners of a small isosceles triangle.

The distances between the silver ions and the oxygen atoms of the framework, and between the silver ions and the oxygen atoms of the water molecules, d(Ag−O1) = 2.452(3) Å and d(Ag−O2) = 2.625(3) Å, respectively, are similar to the corresponding distances in silver zeolite A [$d(Ag-O_{framework})$ = 2.47 Å, $d(Ag-O_{water})$ = 2.57 Å].[14] However, d(Ag−O1) is considerably larger than the corresponding distance in anhydrous silver sodalite $[Ag_3]_2[Al_3Si_3O_{12}]_2$:[11] $d(Ag-O_{framework})$ = 2.347 Å. This is due to the higher coordination number (*c.n.*) of the Ag^+ ions in the hydrated (*c.n.* = 6) versus the anhydrous (*c.n.* = 3) state. Also, the bonding in the anhydrous silver sodalite is more covalent than in the hydrated form. The silver−oxygen bond lengths in SHS and in hydrated silver zeolite A lie in the range found in ionic silver salts with high coordination numbers of Ag^+, e.g. d(Ag−O) = 2.48 Å in $AgNO_3$.

A comparison between the metal−metal, the metal−oxygen and the oxygen−oxygen distances in SHS and in the sodium analogue gives some indications for the cause of the different structural arrangements in these two compounds:

Coordination of the Metal Atoms

In $[Na_3(H_2O)_4]_2[Al_3Si_3O_{12}]_2$, the metal−oxygen distances to the framework oxygen atoms and to those of the water molecules are very similar [$d(Na-O_{framework})$ = 2.51 Å, $d(Na-O_{water})$ = 2.46 Å].[17] This indicates that the Na^+ ions interact with similar strengths with the framework and with the water molecules. The corresponding values for SHS show that the Ag^+ cations prefer coordination to the framework oxygen atoms. This is in line with the general feature of Ag^+ chemistry that interactions between silver cations and water molecules are rare and weak. Consider, for example, the small number of hydrated silver salts. In SHS, the interactions between the water molecules and the non-framework Ag^+ ions are even weaker than in typical hydrates, e.g. $d(Ag-O_{water})$ = 2.46−2.48 Å in $Ag_2IF{\cdot}2\,H_2O$ or $d(Ag-O_{water})$ = 2.35−2.41 Å in $Ag_7I_2F_5 \cdot 2.5\,H_2O$.[18]

Interactions Between the Water Molecules

As in SHS the water molecules can interact only weakly with the non-framework Ag^+ ions, but undergo stronger hydrogen bonding with each other (Figure 3, **b**). Hence, in SHS, the distance d(O2−O2) between the oxygen atoms of the water molecules is only 2.64 Å, which is shorter than the corresponding value in bulk Ice-I_h (2.75 Å). On the contrary, in sodium hydro sodalite, the corresponding interatomic distance amounts to 3.22 Å, indicating only weak hydrogen bonding interactions between the water molecules (Figure 3, **e**).

Interactions Between Metal Cations

Since the work of Jansen,[19] it is well known that the structural chemistry of Ag^+ ions is often determined by relatively short Ag^+-Ag^+ contacts, and a tendency of the Ag^+ ions to segregate into specified regions of the structure, owing to $d^{10}-d^{10}$ interactions. In SHS, the interatomic Ag−Ag distance d(Ag1−Ag2) = 3.27 Å is at the upper limit of the range of distances in which such interactions can be assumed (the Ag−Ag van der Waals distance is ca. 3.4 Å). In contrast to our interpretation, Seff[20] and Gellens[15] assigned this distance unequivocally to Ag^+-Ag^0 bonding.

Summarizing these arguments, it is the general weakness of Ag^+-H_2O relative to Na^+-H_2O interactions that leads to strong hydrogen bonding between the water molecules in SHS and, in turn, to weak interactions between the water molecules and the framework. This effect is corroborated by weak $d^{10}-d^{10}$ interactions between the Ag^+ cations. Correspondingly, the disorder model shows a clear segregation of the metal ions and the water molecules into different parts of the sodalite cage (Figure 3, **b**).

The structural model derived here is consistent with all available experimental data. We wish to emphasise that our results are significantly different from the findings of Ozin et al.,[10] who on the basis of a Rietveld refinement of SHS suggested a structural model similar to that of sodium hydro sodalite.[18] The authors claimed to have detected only one 8*e* Wyckoff position for the Ag^+ cations (with a population parameter of 75%) and one fully occupied 8*e* Wyckoff position for the oxygen atoms of the water molecules. We were not able to reproduce these results of Ozin et al.[10] A Rietveld refinement taking these results as a starting model did not converge. Huge jumps occurred in the *x* parameter of the O2 atom (Δx = 0.05 corresponding to a distance of 0.8 Å); its population parameter increased to 185%. The attempt was stopped at this stage. We therefore conclude that either the silver hydro sodalite prepared by Ozin et al. was of a different nature to that prepared by us, or that their structure refinement is not correct. The synthesis of

the sodium hydro sodalite carried out by Ozin et al. is different to our synthesis, but the analytical data show that both sodalites are very similar apart from the degree of crystallinity. Ozin et al. work at low temperature and at low pressure; under these conditions the crystallinity of the product sodalites is not as high as when prepared under the high-temperature and high-pressure conditions used by us. The ion-exchange procedures were the same in our work and in that of Ozin et al., so that both SHS should be identical, apart from the degree of crystallinity. High cristallinity is of course very important for a reliable Rietveld refinement. Unfortunately, Ozin et al. did not show a powder pattern of the SHS, but they reported that their data for the silver hydro sodalite sample led to a poor refinement of the framework atoms. We therefore assume that the crystal structure and the structural model presented here give a more reliable picture of SHS than does the work of Ozin et al.[10]

Experimental Section

Synthesis and Methods of Characterization

SHS was prepared in a three-step procedure involving the synthesis of the basic sodium hydro sodalite $[Na_4(OH)(H_2O)]_2[Si_3Al_3O_{12}]_2$ in Teflon-lined steel autoclaves followed by Soxhlet extraction with water at 373 K to give the non-basic hydro sodalite $[Na_3(H_2O)_4]_2[Al_3Si_3O_{12}]_2$.[3] Subsequent ion exchange was performed for one day with a 1 N $AgNO_3$ solution at 383 K in Teflon-lined steel autoclaves filled to 90%. The product was washed with distilled water and dried at 333 K. The degree of exchange was determined indirectly by flame photometry of the exchange solution (Na^+ content of the solution after the exchange reaction) and by titration according to Volhard (Ag^+ content of the solution after exchange). The water content was determined using a Netzsch thermoanalyzer STA 429 (N_2 atmosphere, heating rate 10 K/min) combining thermogravimetry (TG), difference thermogravimetry (DTG) and difference thermal analysis (DTA).

The crystallinity of the product and the purity of the compounds were monitored by powder X-ray diffraction employing a Guinier−Huber camera 600 with Cu-$K_{\alpha 1}$ radiation. Scanning electron micrographs were obtained on a JEOL scanning electron microscope (JSM-840A).

IR absorption analysis (KBr pellets) was performed on a Mattson Polaris TM FT spectrometer in the range of 4000 to 400 cm^{-1}.

^1H MAS NMR spectra were recorded at 400.13 MHz on a Bruker MSL-400 NMR spectrometer using a Bruker double-bearing MAS probe with 4-mm zirconia rotors. Single-pulse excitation was applied with a 4-s pulse width (corresponding to a 45° flip angle) and a 5-s pulse repetition. For each spectrum, 16 scans were accumulated at spinning rates of 10 kHz. Spectra simulations were performed using the PC program WINFIT, part of the Bruker WINNMR software package. ^{29}Si MAS NMR spectra were measured at 79.49 MHz using 7-mm rotors with a spinning speed of 4 kHz. Furthermore, 32 scans were recorded with a 3-s pulse width (corresponding to a 35° flip angle) and a 5-s pulse repetition. ^1H and ^{29}Si chemical shifts were related to tetramethylsilane using adamantane and Q_8M_8, respectively, as secondary standards.

X-ray Diffraction Studies

Powder photographs were taken on a Guinier camera (Huber system G600) with Cu-$K\alpha_1$ radiation (internal standard Si). The unit-cell constant of the cubic cell was obtained by LSQS refinement [8.950(2) Å] employing the software package AXES.[21]

Two different XRD patterns of SHS were recorded. The first was collected at room temperature on a Scintag powder diffractometer (Bragg−Brentano geometry) with Cu-$K\alpha$ radiation. The sample was prepared in a flat platinum sample holder which was spun during the measurement. The step width was set to 0.02 °2Θ in the range of 12 °2Θ to 110 °2Θ, resulting in 4900 data points. Some of the data points had to be removed owing to reflections of the platinum sample holder. Therefore only 3910 data points were considered for the refinement (data set 1). Further experimental details are given in Table 4.

The second data set was recorded on a Huber G642 powder camera with Cu-$K\alpha_1$ radiation (Ge monochromator) employing an X-ray sensitive storage film (Hamamatsu H6780). The sample was prepared between two transparent foils (flat sample), and the sample holder was moved tangentially to the focal circle during the measurement. The film was evaluated using a step width of 0.01 °2Θ in the range of 0 °2Θ to 100 °2Θ, resulting in 10 000 data points. During the Rietveld refinement, only data above 12.00 °2Θ were used (8750 data points, data set 2), because no reflections were detected below this value (Figure 6).

Further experimental details are given in Table 4. Both data sets were analysed in a similar way by the XRS-82 program[23] using the Rietveld method. Prior to refinement, the space group of the compound was determined to be *P*-43*n* (No. 218), the background of the pattern was subtracted manually and the contribution of Cu-$K\alpha_2$ radiation in data set 1 was eliminated by employing the algorithm of Ladell et al.[24] Two profile functions were determined employing Baerlocher's Learned Peak-Shape function,[25] one on the (211) reflection (24.204 °2Θ) and one on the (431) reflection (51.753 °2Θ). Atomic scattering factors were taken from reference 17. The least-squares refinement was started with the coordinates of the atoms Al, Si and O1 of the framework structure of ($[Na_3(H_2O)_4]_2[Al_3Si_3O_{12}]_2$).[17] We did not succeed in using the position and the population parameters of the sodium cations of this compound for the Ag^+ cations in SHS. Therefore the positions of the occluded Ag^+ cations and of the oxygen atoms of the water molecules were determined in subsequent difference Fourier syntheses of the electron density and from structural chemical arguments. All peaks detected in the range from 12.00 °2Θ to 100.00 °2Θ were used in the refinement process.

The first difference Fourier synthesis was carried out after the cautious adjustment of some profile parameters (zero-point and peak-asymmetry correction) and the first cautious relaxation of the position of the framework oxygen atoms. It revealed electron density approximately at positions (0.17, *x*, *x*) and (0.31, *x*, *x*) which were first attributed to the positions of the silver cations [(0.17, *x*, *x*), population parameter 0.75] and of the oxygen atoms of occluded water molecules [(0.31, *x*, *x*), population parameter 1.0]. Further refinement included the relaxation of all profile parameters as well as of the atomic positions and displacement parameters of the different atoms. However, release of the population parameter of the occluded silver cations led to a significant decrease below 0.6, while the refinement of the population parameter of the occluded oxygen atom led to a significant increase above 1.2. The silver cations and oxygen atoms were therefore removed from the system and a new difference Fourier synthesis was performed. The calculation again

Table 4. Details of the measurement of powder X-ray diffraction data and Rietveld refinement for $[Ag_3(H_2O)_4]_2[Al_3Si_3O_{12}]_2$

	Data set 1	Data set 2
Powder X-ray data collection	Bragg−Brentano Scintag diffractometer reflection geometry, graphite monochromator, Cu-$K\alpha$ radiation λ_1 = 1.54051 Å and λ_2 = 1.54051 Å Range of measurement: 12° ≤ 2θ ≤ 110° step width 0.02° 2Θ, 93 contributing reflections, 4900 observations	Huber G642 diffraction asymmetric Guinier transmission geometry Ge monochromator, Cu-$K\alpha_1$ radiation λ = 1.54051 Å Range of measurement: 0° ≤ 2θ ≤ 99.5° step width 0.005° 2Θ, selected range for refinement 12.58° ≤ 2θ ≤ 99.50°, step width 0.01° 2Θ, 80 contributing reflections, 8849 observations
	4642 observations used for refinement	8692 observations used for refinement
Number of parameters refined	Profile parameters: 12 Atomic parameters: 10	Profile parameters: 12 Atomic parameters: 10
Number of refined parameters in final cycle	17 (no simultaneous refinement of parameters of the two profile functions)	18 (no simultaneous refinement of parameters of the two profile functions)
R factors	R_F = 0.097 R_{wp} = 0.133, R_{exp} = 0.099 χ^2 = 1.88, $\Delta/\sigma < 0.03$	R_F = 0.069 R_{wp} = 0.090, R_{exp} = 0.066 χ^2 = 1.86, $\Delta/\sigma < 0.03$
Final difference Fourier synthesis	$\Delta\rho_{max}$= +2.0 eÅ^{-3} (in 0.305, 0.014, 0.307)	$\Delta\rho_{max}$= +1.6 eÅ^{-3} (in 0.263, *x*, *x*)
Computer programs	XRS82 software package[23]	XRS82 software package[23]
Atomic scattering factors	taken from ref.[22]	taken from ref.[22]

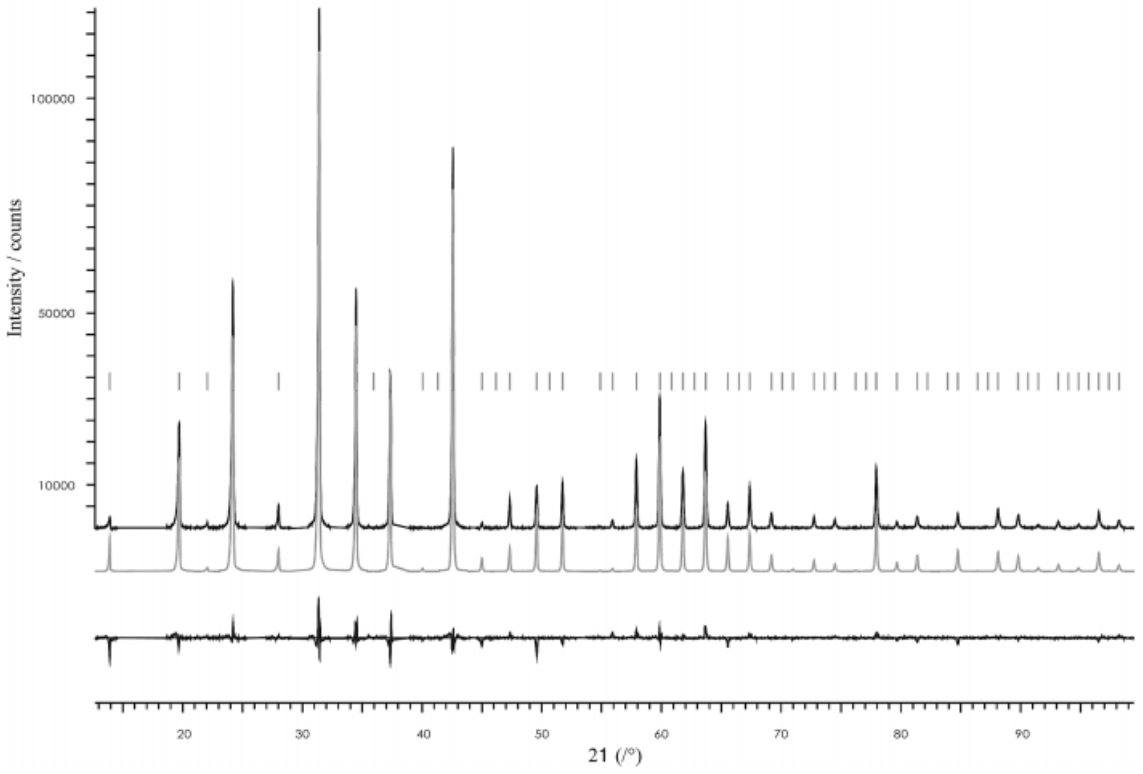

Figure 6. Observed (I_{obs}), calculated (I_{calc}) and difference ($I_{diff} = I_{obs} - I_{calc}$) powder diffraction patterns of $[Ag_3(H_2O)_4]_2[Al_3Si_3O_{12}]_2$ according to the Rietveld refinement

showed electron density at approximately (0.171, *x*, *x*) and at (0.311, *x*, *x*), with an intensity ratio of approximately 2:1. Therefore we concluded, that the silver cations may be located at these two different positions with population parameters of 0.5 for Ag1 and 0.25 for Ag2. After a few refinement cycles, an additional Fourier synthesis revealed remaining electron density at (0.35, *x*, *x*), close to the Ag2 cation. An oxygen atom O2 was placed at position (0.35, *x*, *x*). Taking into account the population parameter of the Ag2 cation (25%), O2 was assigned a population parameter of 75% to avoid very short distances *d*(Ag2−O2). Therefore only six oxygen atoms out of eight could be detected (eight water molecules per formula unit were found by thermal analysis, as shown below). We tested several different structural models in order to find the remaining two oxygen atoms. These models resulted either in very high temperature factors for the additional positions of the oxygen atoms, or unreasonably short distances between the occluded oxy-

gen atoms (shorter than 1.9 A). Therefore, this refinement led to the results given in Table 1−3, with a model containing only one position for the oxygen atoms of the occluded water molecules. In the last refinement cycle of our model, all the position parameters of the occluded atoms as well as all the isotropic displacement parameters were released. Other parameters such as the scaling factor, zero-point shift and peak parameters were released during another cycle. Evaluation of data set 2 followed a similar path and led to similar results. In the two last refinement cycles of the second data set 2, all the parameters were released. (Two refinement cycles were necessary since it is not possible to refine the profile parameters of the two profile functions simultaneously.) All the displacement parameters were treated isotropically. Using anisotropic displacement parameters for the silver cations (which led to a significant improvement in the result of the refinement of ASS[7]) did not lead to any improvement in the present case.

After isotropic refinement of all the atoms, remaining electron densities of approximately $\Delta\rho = 2.0$ $e^{-}Å^{-3}$ at (0.305, 0.014, 0.306) for the first data set and of approximately $\Delta\rho = 1.6$ $e^{-}Å^{-3}$ at (0.26, 0.26, 0.26) for the second set were detected. These positions are close to the centre of the six-membered ring of the framework. However, it was not possible to introduce an atom that could be refined at these positions. Therefore, we regard these electron densities as artefacts (e.g., Hu and Depmeier[26]).

Acknowledgments

We thank Ch. Baerlocher for the measurement of the Bragg−Brentano diffraction pattern. Financial help from the Fonds der Chemischen Industrie is acknowledged.

[1] L. Z. Pauling, *Z. Kristallogr.* **1930**, *74*, 214−216.
[2] J. Felsche, S. Luger, *Thermochim. Acta* **1987**, *118*, 35−55.
[3] G. Engelhardt, P. Sieger, J. Felsche, *J. Am. Chem. Soc.* **1992**, *114*, 1173−1182.
[4] G. A. Ozin, A. Kuperman, A. Stein, *Angew. Chem. Int. Ed. Engl.* **1989**, *28*, 373−390.
[5] A. Stein, G. A. Ozin, G. D. Stucky, *J. Am. Chem. Soc.* **1992**, *112*, 904−905.
[6] A. Stein, G. A. Ozin, G. D. Stucky, *J. Soc. Photogr. Sci. Technol. Japan.* **1990**, *53*, 322−328.
[7] G. A. Ozin, A. Stein, G. D. Stucky, J. Godber, *Inclus. Phenom. Molec. Recogn.* **1990**, 379−393.
[8] A. Stein, P. M. Macdonald, G. A. Ozin, G. D. Stucky, *J. Phys. Chem.* **1990**, *94*, 6943−6948.
[9] A. Stein, G. A. Ozin, P. M. Macdonald, G. D. Stucky, R. Jelinek, *J. Am. Chem. Soc.* **1992**, *114*, 5171−5186.
[10] A. Stein, G. A. Ozin, G. D. Stucky, *J. Am. Chem. Soc.* **1992**, *114*, 8119−8129.
[11] P. Behrens, P. B. Kempa, S. Assmann, M. Wiebcke, J. Felsche, *J. Solid State Chem.* **1995**, *115*, 55−65.
[12] S. Eiden-Assmann, A. M. Schneider, P. Behrens, M. Wiebcke, G. Engelhardt, J. Felsche, *Chem. Eur. J.* **2000**, *6*, 292−297.
[13] G. Engelhardt, D. Michel, *High-Resolution Solid State NMR of Silicates and Zeolites*, Wiley: Chichester, **1987**.
[14] C. M. B. Henderson, D. Taylor, *Spectrochim. Acta* **1979**, *35A*, 929−935.
[15] L. R. Gellens, J. V. Smith, J. J. Pluth, *J. Am. Chem. Soc.* **1983**, *105*, 51−55; L. R. Gellens, W. J. Mortier, R. A. Schoonheydt, J. B. Uytterhoeven, *J. Phys. Chem.* **1981**, *85*, 2783−2788.
[16] M. Jansen, *Angew. Chem. Int. Ed. Engl.* **1986**, *26*, 1098−110.
[17] J. Felsche, S. Luger, Ch. Baerlocher, *Zeolites* **1986**, *6*, 367−372.
[18] M. Molinier, W. Massa, *Z. Anorg. Allg. Chem.* **1994**, *620*, 833−838; K. Persson, B. Holmberg, *J. Solid State Chem.* **1982**, *42*, 1−10.
[19] M. Jansen, *Angew. Chem. Int. Ed. Engl.* **1987**, *26*, 1098; *Angew. Chem.* **1987**, *99*, 1136−1149.
[20] Y. Kim, K. Seff, *J. Phys. Chem.* **1978**, *82*, 1071−1077.
[21] H. Mändar, T. Vajaka, *AXES*, version 1.9A of **1999**.
[22] Th. Hahn, *International Tables for X-ray Crystallography*, Kynoch Press: Birmingham, **1974**; *Vol. IV*, pp. 99, 149.
[23] Ch. Baerlocher, *The X-ray Rietveld System*, version of **1998**.
[24] J. Ladell, A. Zagofsky, S. Pearlman, *J. Appl. Cryst.* **1975**, *8*, 499−506.
[25] A. Hepp, Ch. Baerlocher, *Austral. J. Phys.* **1988**, *41*, 229−236; Ch. Baerlocher, *Proc. 6th Int. Zeolite Conf.*, Reno, USA, 823−829.
[26] X. Hu, W. Depmeier, *Z. Kristallogr.* **1992**, *201*, 99−111.

Received April 28, 2000
[I00168]